Neuro-Oncology 12(4):366–376, 2010.
doi:10.1093/neuonc/nop033
Advance Access publication January 11, 2010

Morphologic and molecular characterization of ATRT xenografts adapted for orthotopic therapeutic testing

Rintaro Hashizume, Nalin Gupta, Mitchel S. Berger, Anu Banerjee, Michael D. Prados, Jennifer Ayers-Ringler, C. David James, and Scott R. VandenBerg

Brain Tumor Research Center (R.H., N.G., M.S.B., A.B., M.D.P., J.A.-R., C.D.J.); Department of Neurological Surgery (R.H., N.G., M.S.B., A.B., M.D.P., J.A.-R., C.D.J.); Department of Pediatrics (N.G., A.B.); Department of Pathology, University of California–San Francisco (J.A.-R.); and Department of Pathology, University of California, San Diego (S.R.V.)

Atypical teratoid rhabdoid tumor (ATRT) is a malignant tumor of the central nervous system that most commonly arises in young children. The aggressive growth and propensity for early dissemination throughout the neuraxis confers a dismal prognosis. Large clinical trials that could test new therapeutic agents are difficult to conduct due to the low incidence of this cancer. For this reason, high throughput preclinical testing with suitable animal models for ATRT would serve a critical need for identifying the most efficacious treatments. In response to this need, we have adapted ATRT cell lines for bioluminescence imaging (BLI) of intracranial (orthotopic) xenografts established in athymic mice. Our results indicate that following supratentorial or infratentorial injection in athymic mice, ATRT cells produce rapidly growing tumors, often with intraventricular spread or neuraxis dissemination. When established as orthotopic xenografts, the tumors predominantly display cells with a rhabdoid-like cellular morphology that show a spectrum of immunophenotypes similar to primary ATRT tumors. To demonstrate the feasibility of this orthotopic ATRT xenograft model for therapeutic testing with correlation to biomarker analysis, we examined the responses of luciferase-modified ATRT cells to temozolomide (TMZ). These xenografts, which highly express MGMT, are resistant to TMZ treatment when compared with an orthotopic glioblastoma xenograft that is MGMT deficient and responsive to TMZ. These data suggest that an orthotopic ATRT xenograft model, in which BLI is used for monitoring tumor growth and response to therapy, should contribute to the identification of effective therapeutics and regimens for treating this highly aggressive pediatric brain tumor.

Keywords: atypical teratoid rhabdoid tumor, xenograft, orthotopic, INI1, bioluminescence

Atypical teratoid rhabdoid tumors (ATRTs) account for as much as 5% of pediatric brain tumors and approximately 10% tumors of the central nervous system (CNS) in infants.[1,2] While varying among collected case descriptions, there is typically a slight male predominance (1.3–1.4). The average age at diagnosis ranges from 17 to 35 months and more than 90% increase before 5 years.[3–6] The histopathology of these polymorphic tumors has been well documented,[4,5,7,8] with hallmark features including a rhabdoid cell population accompanied by varying proportions of cells with neural, epithelial, and/or mesenchymal differentiation. Definitive diagnosis of ATRT is now based on the detection of deletions and/or inactivating mutations of the chromosome 22-localized hSNF5/INI1 tumor-suppressor gene[9,10] in tumor tissue, and/or the absence of nuclear immunoreactivity for the hSNF5/INI1 gene product in the tumor cells.[11,12]

ATRTs are typically refractory to therapies that are more effective for medulloblastomas and supratentorial primitive neuroectodermal tumors and, consequently, ATRTs have a worse prognosis. A recent survey of 37 ATRT patients under the age of 3 years at St. Jude Children's Hospital showed the survival rate of $<10\%$.[13] In another study, based on a retrospective review of a central registry, the median survival for 42

Received March 30, 2009; accepted May 18, 2009.

Corresponding Author: Scott R. VandenBerg, MD, PhD, UCSD Department of Pathology, MC 0612, 9500 Gilman Drive, La Jolla, CA 92093 (scott.vandenberg@ucsf.edu).

ATRT patients was determined as 16 months.[14] Other retrospective reviews show similar dismal outcomes for children afflicted with ATRT.

Conventional treatment of ATRT includes maximal surgical resection with adjuvant chemotherapy, either with or without radiation.[13,14] Approximately half of the ATRT tumors transiently respond to chemotherapy, but chemotherapy alone is rarely curative. Therapeutic responses are commonly compromised by early leptomeningeal dissemination and the inability for gross tumor resection. The early age of presentation for this cancer has typically limited the aggressive use of radiation therapy, further complicating therapeutic options. Even considering the increased morbidity from radiation therapy in children before 36 months, the poor long-term outcomes of ATRT have necessitated new therapeutic protocols that frequently include radiation therapy for these very young patients.[15–18]

The biologic features that confer high-grade malignancy to ATRT also contribute to the ability of these tumors to grow in athymic mice as human tumor xenografts. Despite the relative rarity of this cancer, we, and others,[19] have successfully established ATRT tumorigenic ATRT cell lines. The development of an ATRT xenograft therapeutic test panel is therefore feasible, and such a panel would allow preclinical trials to be conducted in animals. Because a panel would consist of multiple, unique tumors, results from testing several ATRT xenografts would allow one to assess whether a particular treatment approach was generally effective, or limited to specific molecular subtypes of ATRT.

Here we have reported the development and application of orthotopic ATRT xenografts from a primary surgical ATRT specimen and established ATRT cell lines which were modified with a luciferase reporter for bioluminescence imaging (BLI). Our results indicate that supratentorial or infratentorial injection of these cells produces rapidly growing tumors with growth/dissemination patterns and cellular compositions similar to those observed in primary tumors. These xenografts, as models for preclinical testing, can be longitudinally monitored for response to therapy using BLI.

Materials and Methods

Primary ATRT Tissue and Cell Lines

The primary ATRT tumor arose in a 10-month-old male and was a large mass (5.2 × 3.8 × 5.3 cm) located in the left frontal lobe principally involving the caudate and putamen with marked encroachment of the lateral ventricle. Despite intensive chemotherapy with cyclophosphamide, cisplatin, methotrexate, vincristine, etoposide, carmustine, and irinotecan that followed surgical resection, the patient died with progressive tumor growth at 16 months. The ATRT tissue used for engraftment in athymic mice was from the primary tumor resection following the initial diagnosis. Macroscopically pure tumor sample was minced with a scalpel, and then triturated using a sterile pipette. To initiate the xenografts, 100 μL of this tumor tissue suspension was injected subcutaneously (s.c.) into the right flanks of two athymic mice as previously described.[20]

Established ATRT cell lines BT-12 and BT-16 were gifts from Peter Houghton, St. Jude Children's Research Hospital, and were maintained as an exponentially growing monolayer in complete medium consisting of Dulbecco's modified Eagle's medium (DMEM, GIBCO 11965, Invitrogen, Carlsbad, California) supplemented with 10% fetal bovine serum. Cells were cultured at 37°C in a humidified atmosphere containing 95% air and 5% CO_2. For implantation, cells were harvested by trypsinization, washed once, and resuspended in Hanks' Balanced Salt Solution (HBSS) without Ca^{2+} and Mg^{2+}. The GS-2 glioblastoma cell line was developed by Manfred Westphal, Department of Neurosurgery, University Hospital Eppendorf, Hamburg, Germany, and maintained as a neurosphere culture, as previously described.[21] Unique DNA "fingerprint" identities (ie, variable number tandem repeat polymerase chain reaction products) were established for all cell lines used in this study, as well as for the xenografts derived directly from the patient ATRT transplant.

Modification of ATRT Cells with Firefly Luciferase Expressing Reporter

To enable noninvasive monitoring of intracranial tumor growth and response to therapy, BT-12 and BT-16 cells were transduced with HIV-1–based lentiviral vectors expressing firefly luciferase (Fluc) under the control of the spleen focus-forming virus (SFFV) promoter. The optical reporter gene was cloned into the vector plasmid pHRSIN-CSGW-dlNotI. Lentiviral vector was generated by transient transfection of 293T cells with plasmids encoding the vesicular stomatitis virus G envelope, gag-pol, and Fluc genes.[22] Conditioned medium containing viral vectors was harvested 48 hours posttransfection and filtered (0.45 μm), and expression of Fluc was confirmed by measuring cellular luciferase activity.

Animals

Five-week-old female athymic mice (nu/nu genotype, BALB/c background) were purchased from Simonsen Laboratories (Gilroy, California). Animals were housed under aseptic conditions, which included filtered air and sterilized food, water, bedding, and cages. The UCSF Institutional Animal Care and Use Committee approved all animal protocols.

Xenografts of Primary ATRT Tissue and Permanent ATRT Cell Lines

The subcutaneous xenografts that were implanted from the surgical specimen grew to a maximum allowable size (~2000 mm^3) in each mouse by day 50 postinjection. At

this time, the mice were euthanized, with their s.c. tumors immediately resected and processed as follows: (i) flash freezing for subsequent molecular characterization of extracted analytes; (ii) cryopreservation; (iii) formalin fixation and paraffin embedding; and (iv) preparation of cell suspensions as described above for intracranial propagation in a series of 5 mice, and for continued subcutaneous propagation (specimen not propagated as a cell culture). The procedure for supratentorial injection of tumor cell suspensions, derived either from subcutaneous xenograft or from permanent cell lines, is as follows. Rodents were anesthetized with an intraperitoneal injection of a mixture containing 100 mg/kg ketamine and 10 mg/kg xylazine in 0.9% saline. The top of the head of anesthetized rodents was swabbed with Betadine and the skin opened by incision with a scalpel over the middle frontal bone. A small hole in the skull was created by puncture with a sharp 25 gauge needle 3.0 mm to the right of the midline and just behind the bregma. At this depth and location, 5×10^5 cells in 3 μL HBSS without Ca^{2+} and Mg^{2+} were manually injected very slowly (over 1 minute) into the caudate/putamen. All procedures were carried out under sterile conditions. Mice were monitored daily for presentation of neurologic symptoms indicative of tumor burden, at which time they were euthanized, with subsequent resection of brain for formalin fixation and paraffin embedding. For infratentorial (cerebellar) injection of cells, the same procedures were followed except that the injection coordinates used were 3.0 mm to the right of the midline, 1.5 mm behind the lambdoid suture, and 3.0 mm deep from the bottom of the skull.

In Vivo BLI

In vivo BLI was performed with the Xenogen IVIS Lumina System (Xenogen Corp., Alameda, California) coupled to the data-acquisition LivingImage software (Xenogen Corp.). Mice were anesthetized with 100 mg/kg ketamine and 10 mg/kg xylazine and imaged 10 minutes after intraperitoneal injection of luciferin (D-luciferin potassium salt, 150 mg/kg, Gold Biotechnology, St. Louis, Missouri). Signal intensity was quantified within a region of interest over the heads of mice, as defined by the LivingImage software.

Therapy Response Experiments

Procedures used for intracranial tumor therapy–response experiments, including monitoring of tumor growth and response to therapy by BLI, have previously been described.[22] Following the supratentorial injection of tumor cells as described above, mice were either treated with oral suspension vehicle (OraPlus: Paddock Laboratories, Minneapolis, Minnesota) by gavage (control group), or with 100 mg/kg temozolomide (TMZ: obtained as Temodar from Schering-Plough, Kenilworth, New Jersey) in oral suspension vehicle. Treatment was initiated on day 11 (BT-12) or day 15 (BT-16, GS-2) when the intracranial tumors had achieved a log phase growth according to BLI monitoring. For mice receiving intracranial injection of GS-2, a second dose of 100 mg/kg TMZ was administered when BLI analysis indicated tumor re-growth from initial therapy. All mice were monitored twice weekly by BLI and every day for the development of symptoms related to tumor burden, at which time they were euthanized. The Kaplan–Meier estimator was used to generate survival curves, and differences between survival curves were calculated using a log-rank test.

Immunohistochemistry

All tissue was routinely fixed in either phosphate-buffered 4% formalin or Zn–4% formalin, dehydrated by graded ethanol, and embedded in wax (Paraplast Plus, McCormick Scientific, St. Louis, Missouri) using routine techniques. All sections were cut at 5 μm and mounted on Superfrost/Plus slides (Fisher Scientific, Pittsburgh, Pennsylvania). The following antibodies were obtained from commercial sources and used at the following dilutions and incubation times/temperatures: (i) BAF-47 (SNF5): BD Transduction Lab (San Jose, California), #612110 at 1:100, 60 minutes/37°C; (ii) glial acidic fibrillary protein (GFAP): Dako (Carpinteria, California) #Z0334 at 1:2000, 32 minutes/37°C; (iii) epithelial membrane antigen (EMA): Cell Marque Corp. (Rocklin, California), #760-4259 at 1 μg/mL, 60 minutes/37°C; (iv) S100: Ventana Medical Systems (Tucson, Arizona) #760-2523 at 1:1, 60 minutes/42°C; and (v) smooth muscle antigen (SMA): Abcam (Cambridge, Massachusetts) #Ab7818 at 1:400, 32 minutes/37°C. All immunohistochemistry was performed on the Ventana Medical Systems Benchmark XT using either the Ultraview (multimer) detection system for the surgical resection tissue or the iView (Avidin-Biotin) detection system with A-V blocking for the xenograft tissues. Epitope retrieval for all antibodies except S100 and GFAP was performed for 30 minutes in Tris buffer, pH 8, at 90°C; for S100, sections were incubated in citrate buffer, pH 6, for 30 minutes at 90°C; and for GFAP, sections were incubated in an alkaline protease, 0.02 U/mL, for 32 minutes.

Methylation-specific PCR

Analysis of MGMT promoter methylation was performed as described by Esteller et al.[23] PCR products were resolved in 4.5% agarose gels (NuSieve 3:1, Lonza, Inc., Allendale, New Jersey), and were subsequently stained using ethidium bromide.

Immunoblot Analysis

Primary antibodies used for immunoblot analysis were for detection of MGMT (R&D Systems, Minneapolis, Minnesota) or α-tubulin (Sigma-Aldrich, St. Louis,

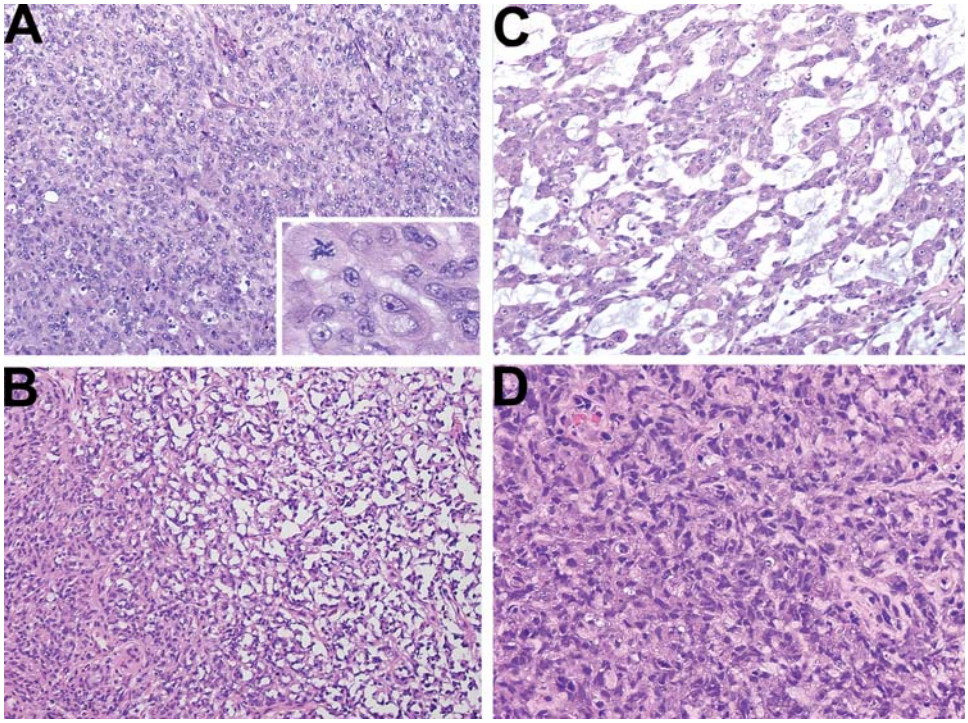

Fig. 1. Histopathologic features of surgical resection specimen. (A) Prominent populations of rhabdoid cells with conspicuous nucleoli and rounded cell bodies with eosinophilic cytoplasm. Mitoses were abundant in these cells (inset). (B) and (C) Mesenchymal differentiation with desmoplastic (B) and myxomatous stroma (C) was present in representative sections. (D) More polymorphous, primitive cells were also present but not conspicuous.

Missouri). Secondary antibodies used were either anti-mouse or anti-goat (Zymed Laboratories, South San Francisco, California).

Results

Primary ATRT Used for Xenograft Establishment

The surgical specimen was red-tan and friable with areas of macronecrosis. Microscopic examination of representative tissue sections showed the histopathologic features that have been well documented for ATRT.[4,7,8] The most abundant cellular component had a rhabdoid cytoarchitecture and was distributed in large sheets or smaller nests (Fig. 1). These were admixed with variable numbers of smaller, more primitive cells or with zones of mesenchymal differentiation. The rhabdoid cells typically had eccentric round nuclei with vesicular chromatin, a large conspicuous nucleolus, and a rounded cell body with eosinophilic cytoplasm. The mesenchymal differentiation with more fusiform cells contained areas of either desmoplastic or myxomatous stroma (Fig. 1). Immunohistochemistry demonstrated the hallmark feature of ATRT with a tumor cell population that, diffusely, was not immunoreactive for BAF-47 (Fig. 2), an epitope of the INI gene product. In addition, there was a conspicuous immunophenotypic diversity of the tumor cells with significant immunoreactivity for GFAP, EMA, vimentin (VIM), SMA, and S100 (Fig. 2).

ATRT Xenografts

Histopathologic analysis of the subcutaneous xenografts of the primary surgical tissue demonstrated a predominance of cells with a rhabdoid cytoarchitecture in densely packed sheets and a loss of mesenchymal differentiation as well as the desmoplastic or myxomatous stroma (Fig. 3). Similar to the primary ATRT, BAF-47 immunoreactivity was absent in all tumor cells (Fig. 4). Orthotopic xenografts, derived from implantation of cells harvested from the subcutaneous tumors, showed similar growth patterns and histopathologic features between infratentorial and supratentorial sites. In both locations, ventricular and/or subarachnoid involvement of tumor was a common feature. The principal patterns of brain invasion were a combination of perivascular spread and dissection of adjacent white matter tracts by small nests of tumor cells with incorporation of reactive brain stroma into the expanding tumor mass (Fig. 3).

The orthotopic xenografts also showed a predominance of the rhabdoid cell population with discrete cell borders and a rounded polygonal cytoarchitecture; however, the larger orthotopic tumors established from short-term cultures of the primary ATRT also contained tumor cells with more prominent cytoplasmic processes (Figs. 3 and 4). The orthotopic xenografts showed immunophenotypic diversity similar to the primary ATRT with preservation of immunoreactivity of EMA, S100, SMA, VIM, and GFAP (Fig. 4). Only the

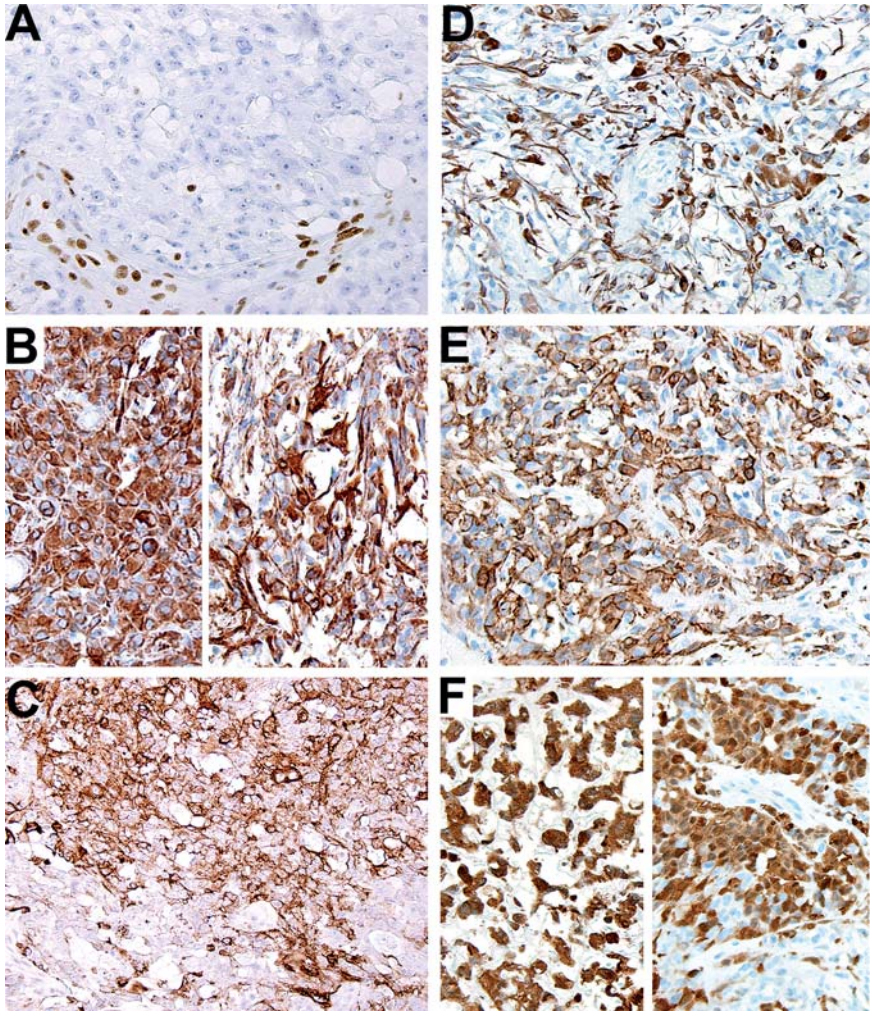

Fig. 2. Immunohistochemistry of surgical resection specimen. (A) All tumor cells lacked BAF-47 immunoreactivity. Note the BAF-47-positive cells in the nonneoplastic vascular and stromal cells. (B) Vimentin immunoreactivity highlighted both the polygonal rhabdoid cells (left) and the more fusiform tumor cells with discrete stout and delicate processes (right). (C) EMA staining was more variable but conspicuous. (D) GFAP immunoreactivity was also present in the polymorphous tumor cell population, including both polygonal cells and cells with conspicuous cellular processes. (E) Immunoreactivity for SMA was a predominant feature in most tissue sections, and (F) S100 staining was present in areas with mxyomatous stroma (left) as well as with the rhabdoid cell population (right).

population of GFAP-immunoreactive cells appeared to be diminished in relation to the primary surgical resection specimen.

Previous studies with glioblastoma (GBM) have demonstrated that tumor propagation as subcutaneous xenografts from primary tumors promotes the retention of EGFR amplification and preservation of tumor invasiveness when implanted into intracranial sites,[21] when compared with cell lines subjected to prolonged cell culture, such as the U87 and D54 GBM lines. To determine whether there are distinct features of orthotopic ATRT established from subcutaneous xenograft vs permanent ATRT cell lines, xenografts arising from injection of BT-12 and BT-16 cells were examined. The intracranial growth patterns and immunohistochemical staining of the xenografts produced from established ATRT cell lines BT-12 and BT-16 were similar to the orthotopic xenografts established from the subcutaneous explants of the primary ATRT, with the exception of a complete lack of SMA and GFAP immunoreactivity (data not shown). Although the composition of SMA and GFAP immunoreactive cells in the founder primary tumors has not been described, a more restricted spectrum of immunophenotypic diversity in ATRT cell lines may be a consequence of extended culture.

Chemotherapy Testing Using ATRT Xenografts

To assess the feasibility of an orthotopic ATRT xenograft approach for therapeutic testing with correlation to tumor biomarkers, a series of 6–10 mice were injected with luciferase-modified BT-12 or BT-16 ATRT cells, as well as with cells from glioblastoma cell line GS-2;[20] half of the mice from each series were administered 100 mg/kg TMZ. All mice were serially monitored by BLI and followed until becoming symptomatic of tumor

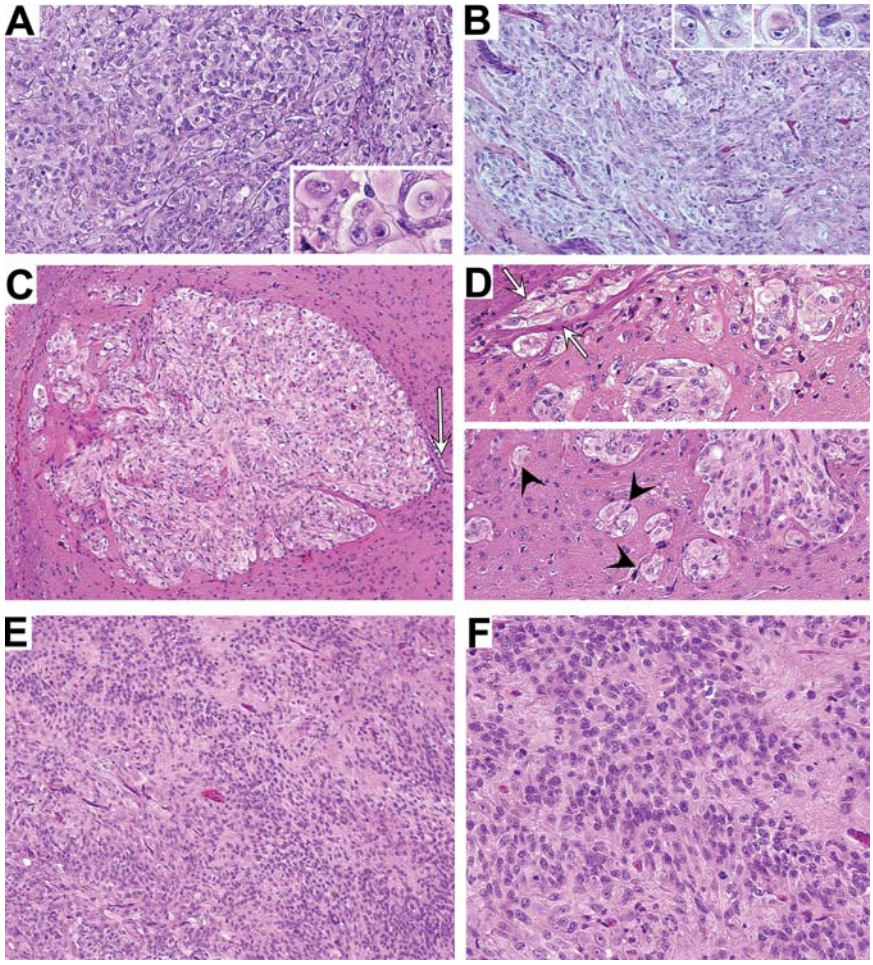

Fig. 3. Xenografts from the primary surgical tissue. Both the subcutaneous (A) and orthotopic (B) xenografts displayed conspicuous populations of rhabdoid cells. (C) Supratentorial xenograft showing ventricular involvement and nodular expansion into adjacent brain. Note the remnant of the ependymal layer (arrow). Higher magnification of another supratentorial tumor (D) shows small nests of perivascular tumor cells (arrow heads) in addition to tumor cells spreading into white matter tracts (arrows). (E) and (F) Larger orthotopic xenografts showed zones of tumor cells with ill-defined cytoplasmic processes.

burden. Results from bioluminescence monitoring indicated progressive growth of untreated tumors for the entire period of observation (Fig. 5A). The responses of the ATRT and GBM orthotopic xenografts to TMZ treatment were markedly distinct. TMZ showed essentially no anti-tumor activity against ATRT, as indicated by the steadily increasing intracranial luminescence of TMZ-treated mice (Fig. 5A), as well as by the similar survival patterns for corresponding treated vs untreated groups (Fig. 5B). In contrast, orthotopic GBM xenografts were responsive to TMZ, as indicated by the sustained suppression of intracranial luminescence of TMZ-treated mice (Fig. 5A), and the corresponding increase in survival of mice receiving TMZ treatment (Fig. 5B). It is notable that intraparenchymal injection of luciferase-modified ATRT cells was commonly followed by the detection of luminescent spinal signal (Fig. 6), in addition to a signal at the primary implantation site. The neuraxis dissemination of these tumor cells is consistent with the frequent ventricular involvement of the orthotopic ATRT xenografts (Fig. 6), which was not observed among mice injected with GS-2 GBM cells.

Methylation-specific PCR analysis of the MGMT gene promoter[23] revealed an absence of methylated promoter in xenografts established from TMZ-resistant BT-12 and BT-16 cell lines, as well as from the primary ATRT surgical specimen and its xenograft derivative. In contrast, the MGMT promoter in TMZ sensitive GS-2 was methylated (Fig. 7A). Corresponding protein extracts showed a lack of detectable MGMT in GS-2 tumors, whereas MGMT expression was readily detectable in all specimens lacking MGMT promoter methylation (Fig. 7B).

Discussion

ATRT was first reported as a distinct clinicopathologic entity more than a decade ago in a well-documented study by Rorke et al.,[7] and was subsequently adopted by the 2000 WHO classification of nervous system

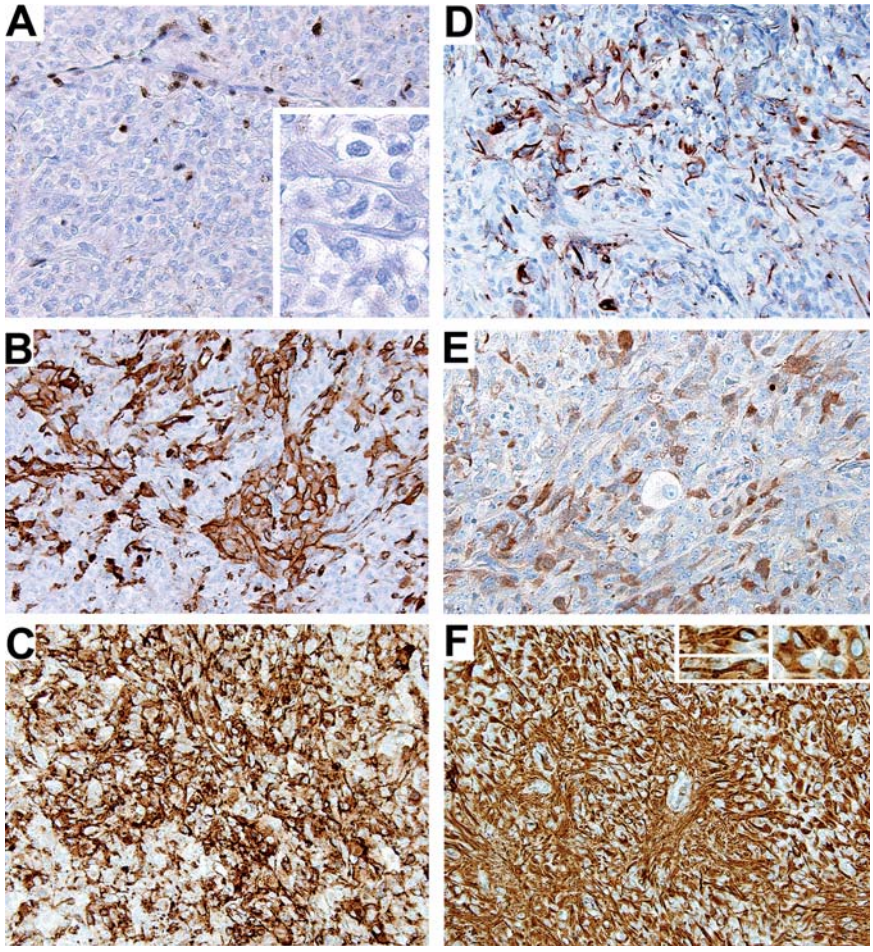

Fig. 4. Immunohistochemistry of xenografts from the surgical tissue. Similar to the primary surgical resection tissue, (A) all tumor cells in the xenografts lacked BAF-47 immunoreactivity (inset, tumor cells at higher magnification). Note the BAF-47-positive cells in the nonneoplastic vascular and stromal cells of the mouse host. Despite the predominance of the more simple pattern of rhabdoid cell sheets in the xenografts compared with the primary surgical specimen, the hallmark feature of immunophenotypic diversity that was present in the primary surgical specimen was maintained in the xenografts as demonstrated by (B) SMA-, (C) EMA-, (D) GFAP-, (E) S100-, and (F) vimentin-reactive cells. The diffuse vimentin immunoreactivity was present in both cells with the typical rhabdoid cytoarchitecture and more fusiform cells with conspicuous stout cytoplasmic processes (inset).

tumors.[24,25] The initial report was followed by several series with more detailed clinical data that documented the highly malignant nature of the tumors and the very poor prognosis, even when aggressive treatment strategies were used. The development of novel, effective therapeutic approaches for ATRT has been hindered by its relative rarity and a lack of specific therapeutic targets in this polymorphic tumor. Data from histoimmunologic studies of ATRT[7,26] suggest that the hallmark rhabdoid cells may constitute a highly malignant, tumor stem cell population that arises from transformation of a multipotential progenitor cell with marked proliferative and invasive features, and the predominance of rhabdoid cellularity in xenografts established from permanent cell lines or from surgical specimens is consistent with this interpretation. The sequence of molecular events that are associated with this transformation is not well understood; however, the genomic lesion that defines ATRT, and that presumptively initiates the process of malignant transformation, is homozygous inactivation of the INI1 gene. This genomic lesion is also common in malignant rhabdoid tumors arising at other body sites in children.[9,27]

The hSNF5/INI1 gene encodes a subunit of ATP-dependent SWI/SNF chromatin remodeling complexes[28] that appear to regulate cell cycling and play critical roles in a variety of differentiation pathways. The core subunit SNF5 appears to function as a tumor suppressor by modulating the transcription of a subset of genes that regulate the balance between cell proliferation and differentiation.[29] This modulation appears to be related to the strengths of the promoter and the degree of chromatin condensation at gene regulatory sites.[27,30] Although the hSNF5/INI1 genomic defect defines a group of malignant rhabdoid tumors at a number of tissue sites,[27] the effects of a specific alteration of hSNF5/INI1 gene combined with tissue-associated epigenomic states[31] are not well understood. The complex

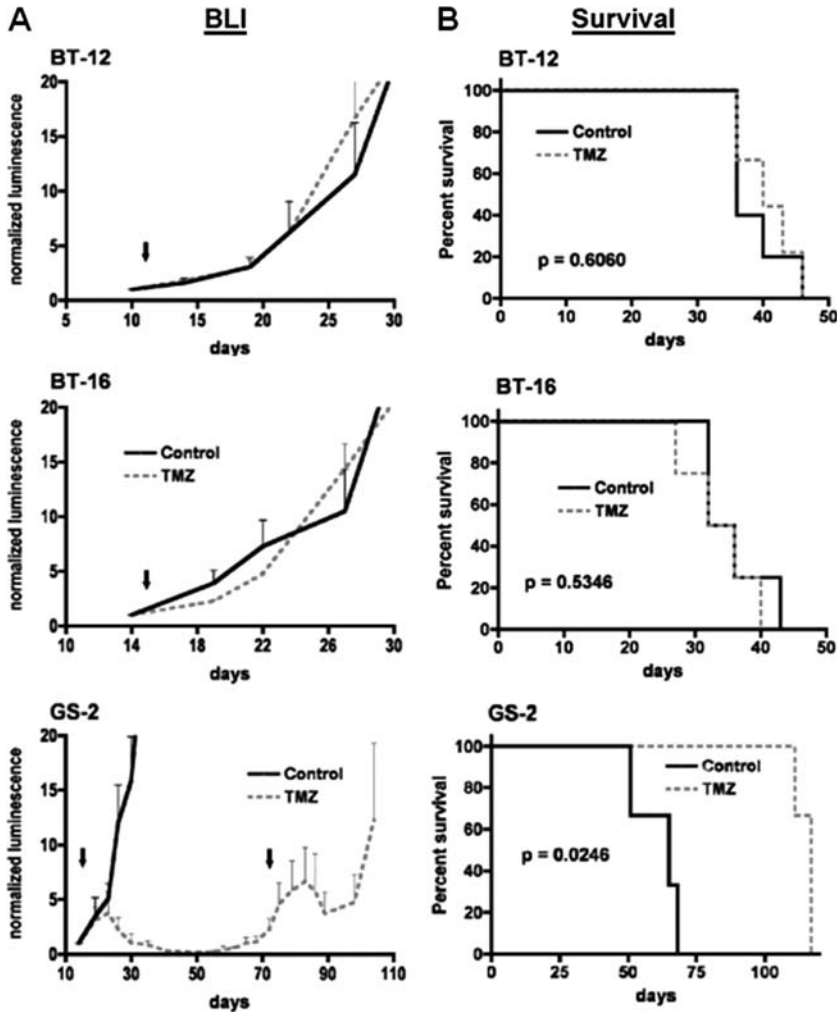

Fig. 5. Bioluminescence (A) and survival (B) analysis of mice receiving intracranial injection of ATRT (BT-12 and BT-16) or GBM (GS-2) cells, and treated with either TMZ or vehicle (control). Bioluminescence monitoring indicates similar growth rates of ATRT orthotopic xenografts following administration of vehicle or of a single 100 mg/kg dose of TMZ (arrows denote day of treatment), whereas mice receiving injection of GBM cells (GS-2) show decreasing luminescence following treatment with TMZ. In fact, GS-2 xenografts show response to a second administration of TMZ at day 71, following indication of tumor re-growth by bioluminescence monitoring. Results from the survival analysis (B) are consistent with the bioluminescence monitoring, showing no survival benefit from TMZ treatment for mice with intracranial ATRT ($P = .6060$ for BT-12, and $P = 0.5346$ for BT-16), whereas TMZ treatment significantly extends the survival of mice with intracranial GS-2 ($P = .0246$)

polymorphic differentiation of MRT arising in the CNS (ie, ATRT) highlights the tissue-specific effects of the INI1 genomic lesions that impact regulation of the cell cycle and of specific differentiation pathways,[29,32–36] and emphasizes the need for ATRT tumor cell–derived experimental systems. These are necessary to define the key pathways that affect the aggressive biological behavior of ATRT and would accordingly reveal potential therapeutic targets.

Studies using cultures of permanent ATRT cell lines, either derived from solid tumors (BT-12, BT-16) or from ATRT tumor cells in the CSF (KCCF),[37–39] have suggested the role of the insulin/insulin growth factor pathways in tumor cell proliferation, survival, and chemosensitivity. In addition, ATRT cell lines have demonstrated in vitro chemosensitivity to inhibitors of histone deacetylase.[40] Only one report has previously documented the culture and primary xenograft implantation of a pediatric ATRT,[41] and this study documented the feasibility of implanting cultured tumor cells into the spinal cord of immunocompromised hosts to produce ATRT-like neoplasms. Whereas the interface between these primary xenograft implantations and the host spinal cords mimicked the aggressive invasive growth pattern of ATRT, the establishment of transplantable ATRT xenografts in nude mice from primary cell cultures was not successful in that study.

The current report compares serially transplantable ATRT xenografts, established from a primary pediatric ATRT, with xenografts established from two permanent ATRT cell lines. Orthotopic ATRT xenografts at either the cerebral or cerebellar sites, regardless

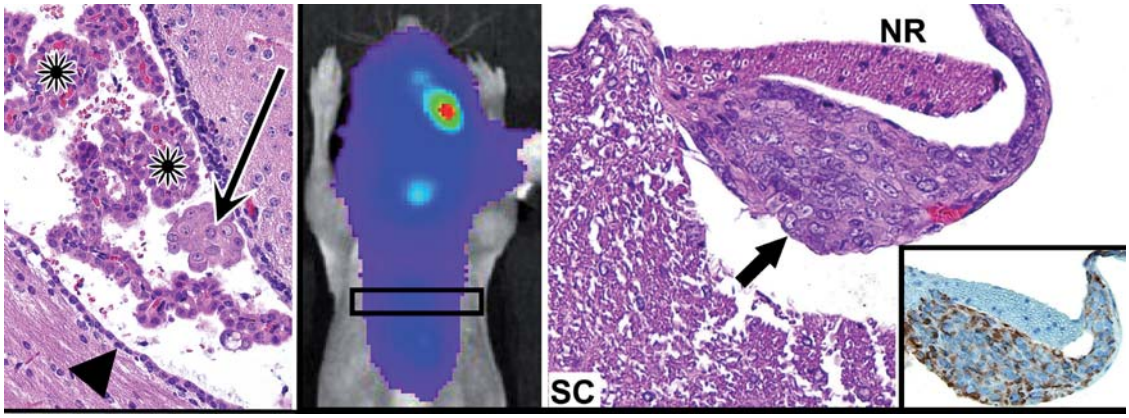

Fig. 6. Spinal dissemination of tumor following supratentorial injection of ATRT xenograft cells. Left: a small nest (arrow) of intraventricular ATRT cells (BT-12) highlights the propensity of the ATRT xenograft cells for intraventricular and neuraxis dissemination. Arrowheads indicate ependyma and asterisks mark nests of host choroid plexus. Middle: mouse having received intracranial injection of luciferase-modified ATRT cells (BT-16) showing luminescence signal along the spinal column. Right: corresponding section from the spinal cord showing leptomeningeal seeding/spread of tumor (arrow) to a spinal nerve root within the subarachnoid space. Lower right: immunoreactivity to human vimentin highlights the tumor (inset). SC, spinal cord; NR, nerve root.

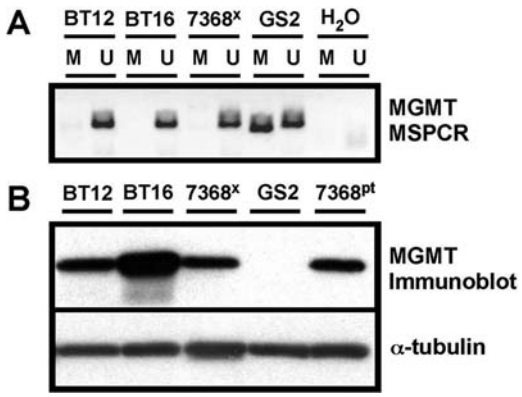

Fig. 7. Analysis of ATRT and GBM for MGMT methylation and expression. (A) Results from methylation-specific PCR show a lack of methylated MGMT promoter in ATRT DNAs (BT-12, BT-16, and 7368 xenograft), whereas DNA from GBM GS-2 shows a PCR product when using methylation-specific primers (M; U denotes reaction product when using primers for unmethylated MGMT promoter). (B) MGMT immunoblot analysis of protein extracts from ATRT cell lines (BT-12 and BT-16), and from paired patient tumor–primary xenograft protein extracts (7368^{pt} and 7368^{x}, respectively). Results show readily detectable MGMT protein in all ATRT specimens, whereas no MGMT protein is detected in the extract from GS-2 cells.

of in vivo or in vitro propagation of tumor cells (ie, in vitro vs in vivo), demonstrated the key biologic features of ATRT. These included a rapid, invasive growth, as well as a propensity for neuraxis dissemination that is similar to the high incidence of ATRT dissemination in patients. Compared with orthotopic GBM xenografts,[21] the ATRT xenografts more frequently spread to intraventricular spaces and subarachnoid zones after intraparenchymal implantation of cells, as documented by histopathologic analysis. Intracranial intraparenchymal injection of ATRT cells was commonly followed by development of luminescent spinal signal, in addition to a signal at the primary implantation site (Fig. 6). In fact, our collective experience with BT-16 has shown that 50% BT-16 cell injections (31 of 62) result in early-neuraxis dissemination, whereas none of a total of 40 GS-2 injections have shown tumor growth outside the brain, in spite of the use of the same coordinates, same number of cells, and same volumes for all intracranial injections. Thus, our study demonstrates the utility of luciferase-modification of ATRT cells for bioluminescence monitoring of neuraxis dissemination of tumor, as well as for monitoring tumor response to therapy.

Modification of ATRT cell lines for BLI produced tumors that resembled the xenografts of primary ATRT cells with respect to histopathology, immunophenotypic diversity, and invasive growth with neuraxis dissemination. The histopathologic features of all the orthotopic xenografts were also similar to the conspicuous predominance of the polygonal rhabdoid-like cells. The histopathologic differences between the xenografts established from the short-term cultures of the primary ATRT tissue and those established from ATRT cell lines after long-term in vitro propagation were subtle and included the absence of more fusiform cells and relative loss of GFAP and SMA immunophenotypes in the tumors established from the BT-12 and BT-16 cells.

Since orthotopic ATRT xenografts in this study recapitulate the invasive growth and CNS dissemination of ATRT in patients, and because modification of these cells for BLI does not affect these properties, we examined the feasibility of an orthotopic ATRT xenograft model for therapeutic testing with correlation to biomarker analysis. For simplicity in testing this paradigm, we examined the responses of luciferase-modified ATRT cells to TMZ. The ATRT xenografts that were tested, which highly express MGMT, are resistant to TMZ treatment with respect to tumor growth and spread when compared with an orthotopic glioblastoma xenograft that is MGMT deficient and responsive to TMZ.

These data suggest that this orthotopic ATRT xenograft model, in which BLI can be used for monitoring, could be used to test new therapeutic regimens with respect to tumor growth and dissemination and, potentially, to expedite the identification of effective treatments for this cancer, in relation to that which can be accomplished through clinical trial activity.

Acknowledgment

The authors are grateful to Tomoko Ozawa for helpful discussion and superb technical assistance.

Conflict of interest statement. None declared.

Funding

This work was supported by NIH grants P50CA097257 (S.R.V., M.S.B., M.D.P., C.D.J.), an Institute Research Award from the Pediatric Brain Tumor Foundation (S.R.V., N.G., M.S.B., M.D.P., and C.D.J.), and an ATRT Project Award from the Pediatric Brain Tumor Foundation (C.D.J.).

References

1. Rickert CH, Paulus W. Epidemiology of central nervous system tumors in childhood and adolescence based on the new WHO classification. *Childs Nerv Syst*. 2001;17:503–511.
2. Lafay-Cousin L, Keene D, Carret A-S, et al. CNS atypical teratoid rhabdoid tumor (ATRT) in children less then 36 months: a Canadian Pediatric Brain Tumor Consortium (CPBTC) experience. Abstracts from the Thirteenth International Symposium on Pediatric Neuro-Oncology, June 29–July 2, 2008, Chicago, Illinois. *Neuro-Oncology*. 2008.
3. Hilden JM, Watterson J, Longee DC, et al. Central nervous system atypical teratoid tumor/rhabdoid tumor: response to intensive therapy and review of the literature. *J Neurooncol*. 1998;40(3):265–275.
4. Packer RJ, Biegel JA, Blaney S, et al. Atypical teratoid/rhabdoid tumor of the central nervous system: report on workshop. *J Pediatr Hematol Oncol*. 2002;24:337–342.
5. Oka H, Scheithauer BW. Clinicopathological characteristics of atypical teratoid/rhabdoid tumor. Neurol Med Chir (Tokyo). 1999;39:510–517.
6. Oka H, Fujii K. Clinical features of atypical teratoid/rhabdoid tumor in Japan. Abstracts from the Thirteenth International Symposium on Pediatric Neuro-Oncology, June 29–July 2, 2008, Chicago, Illinois. *Neuro-Oncology*. 2008.
7. Rorke LB, Packer RJ, Biegel JA. 1996 Central nervous system atypical teratoid/rhabdoid tumors of infancy and childhood: definition of an entity. *J Neurosurg*. 1996;85(1):56–65.
8. Burger PC, Yu IT, Tihan T, et al. Atypical teratoid/rhabdoid tumor of the central nervous system: a highly malignant tumor of infancy and childhood frequently mistaken for medulloblastoma: a Pediatric Oncology Group study. *Am J Surg Pathol*. 1998;22:1083–1092.
9. Biegel JA, Zhou JY, Rorke LB, Stenstrom C, Wainwright LM, Fogelgren B. Germ-line and acquired mutations of INI1 in atypical teratoid and rhabdoid tumors. *Cancer Res*. 1999;59:74–79.
10. Biegel JA, Pollack AI. Molecular analysis of pediatric brain tumors. *Curr Oncol Rep*. 2004;6:445–452.
11. Judkins AR. Immunohistochemistry of INI1 expression: a new tool for old challenges in CNS and soft tissue pathology. *Adv Anat Pathol*. 2007;14:335–339.
12. Takei H, Bhattacharjee MB, Rivera A, Dancer Y, Powell SZ. New immunohistochemical markers in the evaluation of central nervous system tumors: a review of 7 selected adult and pediatric brain tumors. *Arch Pathol Lab Med*. 2007;131:234–241.
13. Tekautz TM, Fuller CE, Blaney S, et al. Atypical teratoid/rhabdoid tumors (ATRT): improved survival in children 3 years of age and older with radiation therapy and high-dose alkylator-based chemotherapy. *J Clin Oncol*. 2005;23:1491–1499.
14. Hilden JM, Meerbaum S, Burger P, et al. Central nervous system atypical teratoid/rhabdoid tumor: results of therapy in children enrolled in a registry. *J Clin Oncol*. 2004;22:2877–2884.
15. Strother D. Atypical teratoid rhabdoid tumors of childhood: diagnosis, treatment and challenges. *Expert Rev Anticancer Ther*. 2005;5:907–915.
16. Meyers SP, Khademian ZP, Biegel JA, et al. Primary intracranial atypical teratoid/rhabdoid tumors of infancy and childhood: MRI features and patient outcomes. *Am J Neuroradiol*. 2006;27:962–971.
17. Chen YW, Wong TT, Ho DM, et al. Impact of radiotherapy for pediatric CNS atypical teratoid/rhabdoid tumor (single institute experience). Int *J Radiat Oncol Biol Phys*. 2006;64:1038–1043.
18. Chi SN, Zimmerman MA, Yao X, et al. Intensive multimodality treatment for children with newly diagnosed CNS atypical teratoid rhabdoid tumor. *J Clin Oncol*. 2009;27:385–389.
19. Houghton PJ, Adamson PC, Blaney S, et al. Testing of new agents in childhood cancer preclinical models: meeting summary. *Clin Cancer Res*. 2002;8:3646–3657.
20. Giannini C, Sarkaria JN, Saito A, et al. Patient tumor EGFR and PDGFRA gene amplifications retained in an invasive intracranial xenograft model of glioblastoma multiforme. *Neuro Oncol*. 2005;7:164–176.
21. Günther HS, Schmidt NO, Phillips HS, et al. Glioblastoma-derived stem cell-enriched cultures form distinct subgroups according to molecular and phenotypic criteria. *Oncogene*. 2008;27:2897–2909.
22. Sarkaria JN, Yang L, Grogan PT, et al. Identification of molecular characteristics correlated with glioblastoma sensitivity to EGFR kinase inhibition through use of an intracranial xenograft test panel. *Mol Cancer Ther*. 2007;6:1167–1174.
23. Esteller M, Garcia-Foncillas J, Andion E, et al. Inactivation of the DNA-repair gene MGMT and the clinical response of gliomas to alkylating agents. *N Engl J Med*. 2000;343:1350–1354.
24. Kleihues, P, Cavenee, WK, eds. World Health Organisation Classification of Tumours: Pathology and Genetics of Tumours of the Nervous System. Lyon: IARC Press; 2000.
25. Kleihues P, Louis DN, Scheithauer BW, et al. The WHO classification of tumors of the nervous system. *J Neuropathol Exp Neurol*. 2002;61:215–225.
26. Bouffard J-P, Sandberg GD, Golden JA, Rorke LJ. Double immunolabeling of central nervous system atypical teratoid/rhabdoid tumors. *Mod Pathol*. 2004;17:679–683.
27. Biegel JA, Tan L, Zhang F, Wainwright L, Russo P, Rorke LB. Alterations of the hSNF5/INI1 gene in central nervous system atypical teratoid/rhabdoid tumors and renal and extrarenal rhabdoid tumors. *Clin Cancer Res*. 2002;8:3461–3467.

28. Versteege I, Medjkane S, Rouillard D, Delattre O. A key role of the hSNF5/INI1 tumour suppressor in the control of the G1-S transition of the cell cycle. *Oncogene.* 2002;21:6403–6412.
29. Caramel J, Medjkane S, Quignon F, Delattre O. The requirement for SNF5/INI1 in adipocyte differentiation highlights new features of malignant rhabdoid tumors. *Oncogene.* 2008;27:2035–2044.
30. Biegel JA, Kalpana G, Knudsen ES, et al. The role of INI-1 and the SWI/SNF complex in the development of rhabdoid tumors: meeting summary from the workshop on childhood atypical teratoid/rhabdoid tumors. *Cancer Res*. 2002;62:323–328.
31. Muhlisch J, Schwering A, Grotzer M, et al. Epigenetic repression of RASSF1A but not CASP8 in supratentorial PNET (sPNET) and atypical teratoid/rhabdoid tumors (AT/RT) of childhood. *Oncogene.* 2006;25:1111–1117.
32. Oruetxebarria I, Venturini F, Kekarainen T, et al. p16INK4a is required for hSNF5 chromatin remodeler-induced cellular senescence in malignant rhabdoid tumor cells. *J Biol Chem*. 2004;279:3807–3816.
33. Daniel Y, Wu DY, Tkachuck DC, et al. The human SNF5/INI1 protein facilitates the function of the growth arrest and DNA damage-inducible protein (GADD34) and modulates GADD34-bound protein phosphatase-1 activity. *J Biol Chem*. 2002;277:27706–27715.
34. Cao Y, Cairns BR, Kornberg RD, Laurent BC. Sfh1p, a component of a novel chromatin-remodeling complex, is required for cell cycle progression. *Mol Cell Biol*. 1997;17:3323–3334.
35. Zhang ZK, Davies KP, Allen J, et al. Cell cycle arrest and repression of cyclin D1 transcription by INI1/hSNF5. *Mol Cell Biol*. 2002;22:5975–5988.
36. Betz BL, Strobeck MW, Reisman DN, Knudsen ES, Weissman BE. Re-expression of hSNF5/INI1/BAF47 in pediatric tumor cells leads to G1 arrest associated with induction of p16ink4a and activation of RB. *Oncogene*. 2002;21:5193–5203.
37. Narendran A, Coppes L, Jayanthan A, et al. Establishment of atypical-teratoid/rhabdoid tumor (AT/RT) cell cultures from disseminated CSF cells: a model to elucidate biology and potential targeted therapeutics. *J Neurooncol*. 2008;90:171–180.
38. D'Cunja J, Shalaby T, Rivera P, et al. Antisense treatment of IGF-IR induces apoptosis and enhances chemosensitivity in central nervous system atypical teratoid/rhabdoid tumours cells. *Eur J Cancer.* 2007;43:1581–1589.
39. Arcaro A, Doepfner KT, Boller D, et al. Novel role for insulin as an autocrine growth factor for malignant brain tumour cells. *Biochem J.* 2007;406:57–66.
40. Furchert SE, Lanvers-Kaminsky C, Juurgens H, Jung M, Loidl A, Fruhwald MC. Inhibitors of histone deacetylases as potential therapeutic tools for high-risk embryonal tumors of the nervous system of childhood. *Int J Cancer*. 2007;120:1787–1794.
41. Yachnis AT, Neubauer D, Muir D. Characterization of a primary central nervous system atypical teratoid/rhabdoid tumor and derivative cell line: immunophenotype and neoplastic properties. *J Neuropathol Exp Neurol*. 1998;57:961–971.